

**Sea salt aerosol
refractive indices**

R. Irshad et al.

Laboratory measurements of the optical properties of sea salt aerosol

R. Irshad¹, R. G. Grainger¹, D. M. Peters¹, R. A. McPheat², K. M. Smith², and G. Thomas¹

¹Atmospheric, Oceanic and Planetary Physics, Clarendon Laboratory, University of Oxford, UK

²Space Science and Technology Department, Rutherford Appleton Laboratory, Didcot, UK

Received: 24 August 2007 – Accepted: 29 September 2007 – Published: 4 January 2008

Correspondence to: R. Irshad (rirshad@atm.ox.ac.uk)

Title Page

Abstract

Introduction

Conclusions

References

Tables

Figures

◀

▶

◀

▶

Back

Close

Full Screen / Esc

Printer-friendly Version

Interactive Discussion

EGU

Abstract

The extinction spectra of laboratory generated sea salt aerosols have been measured from 1 μm to 20 μm using a Bruker 66v/S FTIR spectrometer. Concomitant measurements include temperature, pressure, relative humidity and the aerosol size distribution. The refractive indices of the sea salt have been determined using a simple harmonic oscillator band model (Thomas et al., 2004) for aerosol with relative humidities between 0.1% to 100% sea salt. The resulting refractive index spectra show significant discrepancies when compared to existing sea salt refractive indices.

1 Introduction

Atmospheric aerosols cause direct and indirect forcing of the atmosphere's radiation budget. Aerosol particles may act as cloud condensation nuclei and affect the lifetime of clouds (Penner et al., 2001; Lohmann and Feichter, 2005) or they can influence radiative transfer by scattering and absorbing solar radiation (IPCC, 2007). The optical properties of aerosols are particularly important as they are required to perform radiative transfer calculations in global climate models and allow the radiative effect of such aerosols to be estimated (Hess et al., 1998; Dobbie et al., 2003). In fact the need for refined optical aerosol models for improving satellite retrieval algorithms has been identified by many authors (Torres et al., 1998; King et al., 1999; Dubovik et al., 2002).

Marine aerosols provide a significant contribution to the aerosol environment due to the large source area of the oceans, which cover approximately 70% of the Earth's surface. Sea salt aerosol (SSA) is a component of marine aerosol made up of seawater and dry sea salt particles, and is produced by any mechanism releasing spray from the sea surface. As well as acting as cloud condensation nuclei (Twomey and McMaster, 1955) SSA can also act as a sink for condensable gases, affecting the deposition rate of nitrogen in the form of ammonia to the ocean and thus possibly inhibiting the formation of other aerosol particles (Savoie and Prospero, 1982). Coarse SSA parti-

Sea salt aerosol refractive indices

R. Irshad et al.

Title Page

Abstract

Introduction

Conclusions

References

Tables

Figures

◀

▶

◀

▶

Back

Close

Full Screen / Esc

Printer-friendly Version

Interactive Discussion

cles cause corrosion and are a main contributor to ocean-atmosphere fluxes of organic substances, electric charge, micro-organisms etc. SSA also plays a part in the atmospheric cycles of chlorine and other halogens (Finlayson-Pitts and Hemminger, 2000). Finally, recent observations suggest that the majority of accumulation mode aerosols in the marine boundary layer ($0.1 \mu\text{m} < \text{Radius} < 1 \mu\text{m}$) contain sea salt, and that this sea salt aerosol is responsible for the majority of aerosol-scattered light (Murphy et al., 1998).

For the lowest tens of metres above the ocean, SSA particles usually exist in liquid form. Above this height, at relative humidities (RH) between 45% and 75%, SSA particles may be in either liquid droplet or dry salt form depending on the relative humidity of the particle on creation. As SSA particles are usually formed as liquid droplets, and the RH rarely drops to below 45%, it may be assumed that they always exist as liquid solution drops in the atmosphere (Lewis and Schwartz, 2004).

The refractive indices of sea salt have previously been obtained using reflectance and transmittance measurements made on bulk samples (Volz, 1972). These were made using pellets of KBr with a layer of powdered sea salt pressed onto the surface, and not using actual aerosol. There is also some ambiguity as to whether or not the pellets remained dry during measurement.

Currently, the refractive indices of wet SSA are calculated using mixing rules, i.e. taking a weighted average of the refractive indices of water and dry sea salt (Shettle and Fenn, 1979). While this method may be valid for solid particles suspended in water, it may not hold for solutions of salts such as sodium chloride, which readily dissolve in water. The salts dissociate into separate ions when dissolved in water, for example, sodium chloride dissociates to Na^+ and Cl^- ions. Therefore, the values of refractive index of sea salt used in current climate and retrieval models may not be physically realistic. There is therefore a pressing need for measurements of the optical properties of SSA to quantify and improve on the accuracy of those currently in use.

Previous methods of determining optical properties of aerosol substances include aerosol extinction spectroscopy from small particles and thin films. Refractive index

**Sea salt aerosol
refractive indices**

R. Irshad et al.

Title Page

Abstract

Introduction

Conclusions

References

Tables

Figures

◀

▶

◀

▶

Back

Close

Full Screen / Esc

Printer-friendly Version

Interactive Discussion

is then calculated from extinction measurements using a Kramers-Kronig method that has been described extensively in literature (Milham et al., 1981; Clapp et al., 1995). In this case thin film techniques were rejected due to the possibility of heterogeneous nucleation and interaction with a substrate.

5 Transmittance measurements were undertaken using Fourier-transform-infra-red (FTIR) spectroscopy and the resulting spectra were converted to complex refractive indices over a range of wavelengths using a classical damped harmonic oscillator (CDHO) model, to fit the shape of absorption bands, combined with a Mie scattering algorithm (Thomas et al., 2004). The resulting refractive index spectra are presented in
10 this paper and, where possible, compared with current data from HITRAN (Rothman, 2005).

2 Methodology

Sea salt crystals were dissolved in analytical reagent grade water to make a salt solution. Maldon sea salt was used: this is obtained by evaporation of seawater collected
15 from the east coast of England. As the ratio of the major constituents of sea water are thought to vary minimally with geographical location (Culkin, 1965; Wilson, 1975; DOE, 1994; Lewis and Schwartz, 2004), these salt crystals may be considered representative of the sea salt in the atmosphere. Seawater samples were not used due to likely presence of contaminants that would be evident in the spectral measurements.

20 The salt solution was aerosolised using an OMRON NE-U17 ultrasonic nebuliser. The aerosol was transported in a buffer flow of nitrogen gas and dried using diffusion dryers (Blackford and Simons, 1986). The dry aerosol was then carried into a 2 l glass conditioning vessel where the RH of the aerosol was varied by the introduction of water vapour from a heated water bath. The conditioner was of a sufficient volume to allow
25 the aerosol particles to grow to a stable size before entering the aerosol cell. This is a double-walled stainless steel cell with length 25 cm and internal volume approximately 145 cm³.

Sea salt aerosol refractive indices

R. Irshad et al.

Title Page

Abstract

Introduction

Conclusions

References

Tables

Figures

◀

▶

◀

▶

Back

Close

Full Screen / Esc

Printer-friendly Version

Interactive Discussion

**Sea salt aerosol
refractive indices**

R. Irshad et al.

Title Page

Abstract

Introduction

Conclusions

References

Tables

Figures

◀

▶

◀

▶

Back

Close

Full Screen / Esc

Printer-friendly Version

Interactive Discussion

The aerosol cell was mounted horizontally an evacuated chamber attached to a Bruker 66V/s Fourier transform spectrometer. Here, intensity measurements were made over a range of wavenumbers. Particle size and number density measurements were also made using a GRIMM Sequential Mobility Particle Sizer plus Counter (SMPS+C) and an API Aerosizer instrument (an aerodynamic particle sizer).

Background spectra were recorded to account for the spectral response of the Fourier transform spectrometer and any artefacts introduced by the windows of the optical cell. A Kalman smoother (Kalman, 1960; Maybeck, 1979) was used to match an appropriate background spectrum to each aerosol measurement, and the transmission spectra were calculated using the following equation:

$$T_c(\nu) = \frac{I(\nu)}{I_0(\nu)} \quad (1)$$

where $I_0(\nu)$ is the background intensity, $I(\nu)$ is the sample intensity and $T_c(\nu)$ is the transmission.

Transmission measurements of sea salt aerosol were obtained from 500 to 8000 cm^{-1} at a number of different RH values (Table 1). Several spectral measurements were taken at each RH value and averaged to obtain the final transmission spectrum. The error on these final spectra was estimated by calculating the variance of each spectral point in time from the original averaged data. The transmission data was then processed to retrieve the complex refractive index. The error for each measurement was also updated during the retrieval process to add the uncertainty for each parameter in the model to the measurement error.

Some of the transmission spectra showed evidence of contamination by gas lines of carbon dioxide and water. These were modelled and removed using an iterative non-linear least squares fit retrieval (Rodgers, 2000). However, in some of the spectra, particularly at high RH values, there is still evidence of some remaining lines. This leads to increased uncertainty in the areas where water lines are expected for these spectra.

3 Results

3.1 Classical damped harmonic oscillator model

The final transmission spectrum was used to derive the complex refractive index using a CDHO model after [Thomas et al. \(2004\)](#). In this method, the molecular absorption of aerosol molecules is modelled using a CDHO model that provides a best estimate of the shape of the absorption bands. A Mie scattering algorithm is then used in conjunction with the CDHO model to fully describe the absorption spectrum ([Grainger et al., 2004](#)). The final model of the spectrum is fitted to measurements using a numerical optimal estimation algorithm and the complex refractive index is retrieved. Concomitant measurements of size and number density were used as a priori information for the retrieval. Final retrieved parameters are shown in Table 1.

As the absorption band parameters contain information about the composition of the aerosol compound the ideal a priori band set would be defined by infrared absorption features of component compounds of the aerosol. However, this information was not available in the literature. The most reliable method of obtaining the a priori band set therefore entailed inclusion of expected absorption bands from prior knowledge, and the addition and removal of subsequent bands based on a trial and error method. Table 2 shows the set of band parameters for 70% RH sea salt aerosol. As the RH of the aerosol increased, the size and width of the parameters corresponding to water bands increased. Similarly, as the RH decreased, the size and width of the water bands decreased until they disappeared for the dry sea salt aerosol.

3.1.1 Refractive index retrieval

The retrieval algorithm fits extinction curves calculated from the measured data. Figure 1 shows the extinction calculated from measurements of dry sea salt aerosol compared with the extinction from previous values of dry sea salt refractive indices. The latter data are obtained from the HITRAN database ([Rothman, 2005](#)) and are based on

Title Page

Abstract

Introduction

Conclusions

References

Tables

Figures

◀

▶

◀

▶

Back

Close

Full Screen / Esc

Printer-friendly Version

Interactive Discussion

measurements taken by Volz (1972), and calculations performed by Shettle and Fenn (1979).

The results of the refractive index retrieval for dry sea salt aerosol are shown in Fig. 2. The results show that the retrieved values of the imaginary part, k , the refractive index, follow the shape of the HITRAN data but the experimental data reveal an additional peak at $\sim 1300\text{ cm}^{-1}$. The overall magnitude of the imaginary part is much larger than that of the HITRAN data, up to $\sim 7000\text{ cm}^{-1}$. The retrieved spectrum also shows greater detail than the HITRAN data due to a higher resolution. However, the real part of the refractive index, m , from the experimental data looks very different to that presented by HITRAN. These data were originally obtained by reflectance measurements (Volz, 1972), rather than from transmittance measurements.

The retrieved refractive index data for sea salt aerosols of approximately 50% and 90% RH are shown in Figs. 3 and 4. A clear decrease in the values of the real part of the refractive index at large wavenumbers is observed as the RH increases. Again, the general trend of the variation of refractive index with wavenumber is similar for both data sets in that peaks occur at approximately the same wavenumber values. However, there are significant differences in the size and shapes of these peaks, and the overall magnitude of the real part of the refractive index is consistently greater in the experimental data when compared to the HITRAN data.

4 Discussion

4.1 Comparison with HITRAN data

There is a clear similarity between the two extinction curves shown in Fig. 1. However, the HITRAN data consist of far fewer points and, possibly as a result of this lower resolution, do not show the peak at $\sim 1300\text{ cm}^{-1}$ which is evident in the experimental data. The peaks at $\sim 1625\text{ cm}^{-1}$ and $\sim 3430\text{ cm}^{-1}$ are also much larger in the HITRAN data. The positions of these peaks correspond to the positions of peaks expected due

Sea salt aerosol refractive indices

R. Irshad et al.

Title Page

Abstract

Introduction

Conclusions

References

Tables

Figures

◀

▶

◀

▶

Back

Close

Full Screen / Esc

Printer-friendly Version

Interactive Discussion

to water features. This suggests that the sea salt pellets used to make these measurements were not completely dry. Any subsequent calculations made using these values for dry sea salt would therefore also be incorrect. In addition, the extinction curve of the HITRAN data tends towards a much lower value at high wavenumbers than for the experimental data.

To further investigate the discrepancies between the data sets, attempts were made to retrieve band parameters from the refractive index data from HITRAN. It was anticipated that these would provide the basis of a priori information for retrievals from sea salt experimental data. These attempts proved unsuccessful, indicating that the real and imaginary parts of the refractive index data from HITRAN did not correspond according to the equations used to relate these parameters in the CDHO model (Thomas et al., 2004).

A priori information was then obtained from particle size and number density measurements made during the experiments, and the refractive indices of dry sea salt aerosol were retrieved (Fig. 2). As it had been concluded that the real and imaginary parts of the refractive index data from HITRAN did not correspond, the significant differences between the experimental and HITRAN data for the real part of the refractive index for dry sea salt are unsurprising. The new retrieved real values are relatively constant, although slight disturbances are observed at the wavenumber values where peaks are evident in the HITRAN data. Two of these peaks are expected to be the result of water at $\sim 1625\text{ cm}^{-1}$ and $\sim 3430\text{ cm}^{-1}$, and these were evident in the extinction graph (Fig. 1). Once more, there is a feature at $\sim 1300\text{ cm}^{-1}$ in both the real and imaginary parts of the refractive indices that suggests the presence of a peak undetected by the HITRAN data. The greatest difference between the new data and the current HITRAN data is the increased magnitude of the real part of the new data. A similar increase in magnitude is seen in the imaginary part of the new data; however, in this case, both the new and the current HITRAN data tend to zero at $\sim 7000\text{ cm}^{-1}$.

The measured refractive indices of 50% and 90% RH sea salt aerosol are shown in Figs. 3 and 4 respectively for further comparisons with the current data from HITRAN.

**Sea salt aerosol
refractive indices**

R. Irshad et al.

Title Page

Abstract

Introduction

Conclusions

References

Tables

Figures

◀

▶

◀

▶

Back

Close

Full Screen / Esc

Printer-friendly Version

Interactive Discussion

**Sea salt aerosol
refractive indices**

R. Irshad et al.

Title Page

Abstract

Introduction

Conclusions

References

Tables

Figures

◀

▶

◀

▶

Back

Close

Full Screen / Esc

Printer-friendly Version

Interactive Discussion

Once again the magnitude of both parts of the measured refractive indices are greater than the magnitude of the current data, although this difference becomes smaller as the RH increases. At 50% RH the peaks of the real part of the HITRAN data are greater in amplitude and better defined than those of the new measurements, suggesting a greater level of water than in the aerosol produced for the new measurements. The HITRAN data also show a peak at $\sim 400\text{ cm}^{-1}$ in the real part of the refractive index that is not present in the new measurements. However, this peak does appear in the new measurements of 90% RH sea salt aerosol, suggesting that it is due to a high water content. The new 90% RH measurement also shows much more structure in both the real and imaginary parts than the current HITRAN data. The peaks at $\sim 1625\text{ cm}^{-1}$, $\sim 2000\text{ cm}^{-1}$ and $\sim 3430\text{ cm}^{-1}$ are all attributable to water, and the increased resolution of the new measurements compared to that of the original Volz (1972) measurements allows the structure of the peaks to be better defined. However, the scattering of data points around $\sim 1625\text{ cm}^{-1}$ in the new data indicates remnants of water lines that may provide an additional source of error. Therefore more work is necessary to improve the method of eliminating gas lines. The amplitude of these water peaks is much greater in the new measurements than in the HITRAN data. Also the large O-H stretch feature at $\sim 3330\text{ cm}^{-1}$ in the HITRAN data is centred at the slightly higher wavelength of $\sim 3430\text{ cm}^{-1}$, although the positions of the remaining peaks remain unchanged between the two data sets. Currently the O-H stretch feature is modelled using a number of overlapping bands. This is due to limitations of the CDHO model that require absorption bands to be symmetric. However, it is anticipated that further work on the model may include an asymmetry parameter to better model this feature.

The differences between the new measurements and the current data are attributed to the inaccuracy of the volume weighting model used to calculate the refractive indices in the HITRAN data. The possible presence of water and the apparent inconsistencies between the real and imaginary parts of this refractive index data is also a source of error. The retrievals of water lines from the new measurements of dry sea salt aerosol indicate a relative humidity value of 0.4%, which is assumed to be negligible

for this analysis as minimal water features are observed in the retrieved refractive index spectrum.

4.2 Variation with increasing relative humidity

At high wavenumbers, the real part of the refractive index for sea salt aerosol tends towards a constant value (Figs. 2, 3 and 4). As the aerosol becomes wetter, this value decreases (Figs. 3 and 4). This is to be expected as more water is present in the aerosol and so its refractive index should become closer to that of water (1.33). This is particularly noticeable in the variation of the refractive index at infinite frequency (m_{inf}) shown in Fig. 5.

Figures 6a to b show the retrieved refractive index spectra for sea salt aerosol at various different RH values. It can be seen that, in the real part of the refractive index, the size of the O-H stretch feature at $\sim 3430 \text{ cm}^{-1}$ increases with RH, as does the size of the peak at $\sim 1625 \text{ cm}^{-1}$. The imaginary part of the refractive index exhibits similar trends. The peak due to the O-H stretch from water at $\sim 3430 \text{ cm}^{-1}$ grows significantly larger in amplitude as the RH increases, as does the peak at $\sim 1625 \text{ cm}^{-1}$. However, the peak at $\sim 1800 \text{ cm}^{-1}$ becomes smaller as RH increases, suggesting that it is due to the sea salt rather than water. The trough at $\sim 800 \text{ cm}^{-1}$ in the real part of the data becomes deeper and more defined as the RH increases and the peak at $\sim 400 \text{ cm}^{-1}$ begins to appear.

4.3 Volume mixing rules

The calculations performed by Shettle and Fenn (1979) used sea salt data from Volz (1972) and water refractive indices from Hale and Query (1973). Further and more comprehensive measurements have been made of the refractive indices of water, most recently by Segelstein (1981). To confirm that the discrepancy between the new measurements and the refractive indices calculated by Shettle and Fenn (1979) are not merely due to inaccurate data for water, the volume mixing calculations are repeated

Sea salt aerosol refractive indices

R. Irshad et al.

Title Page

Abstract

Introduction

Conclusions

References

Tables

Figures

◀

▶

◀

▶

Back

Close

Full Screen / Esc

Printer-friendly Version

Interactive Discussion

here using the new measurements of dry sea salt aerosol, and the Segelstein (1981) data for the refractive indices of water. The refractive index spectrum for 70% RH sea salt aerosol was calculated using the volume weighting formula (following Shettle and Fenn, 1979):

$$n = n_w + (n_0 + n_w) \left[\frac{r_0}{r(a_w)} \right] \quad (2)$$

where n_0 is the refractive index of dry sea salt aerosol, n_w is the refractive index of water, r_0 is the dry aerosol particle size and $r(a_w)$ is the size of the wet sea salt aerosol for which the refractive index is required. The calculated refractive indices are compared with the new measurements in Fig. 7. It is clear that, while the positions and shapes of the peaks are similar, the two refractive index spectra are sufficiently different that it may be assumed that the volume mixing rules used to calculate refractive index for wet aerosols provide an inaccurate result compared to direct measurements. This is expected as the dissociation of salt ions upon dissolution of the salt means that the resulting solution cannot merely be considered as a mixture of whole salt particles and water.

5 Conclusions

The refractive indices of sea salt aerosol have been obtained for a range of relative humidity values. A single set of measurements was previously made by Volz (1972). In these measurements the real and imaginary parts of the refractive index were derived by two different measurements: the real part using transmission measurements and the imaginary part using reflectance measurements, both from dry, bulk samples. We found that the real and imaginary parts of the refractive indices from these measurements did not correspond according to the CDHO model.

The refractive indices for wet sea salt aerosols were previously calculated using a volume weighting formula, the Volz (1972) refractive index data for sea salt and refractive index data for water that have since been superceded. Calculations performed

Sea salt aerosol refractive indices

R. Irshad et al.

Title Page

Abstract

Introduction

Conclusions

References

Tables

Figures

◀

▶

◀

▶

Back

Close

Full Screen / Esc

Printer-friendly Version

Interactive Discussion

using the new refractive index data for sea salt and more recent data for the refractive indices of water are inconsistent with each other, suggesting the volume mixing rules are inadequate for describing the refractive indices of solutions.

The results presented here have been retrieved from direct measurements of aerosols and are therefore more representative of the natural aerosol than previous data. This means that the infra-red scattering and absorption of sea salt aerosols can now be more accurately predicted, and more realistic parameters may be used in atmospheric models. Possible further work may involve improving the retrieval of gas lines from transmission spectra to improve accuracy in the spectral regions where water is expected, as well as extending the CDHO method to allow for the presence of asymmetry in the absorption bands.

Acknowledgements. Thanks are due to A. Clack, D. Constable, A. Dudhia, J. Perry, P. Read, J. Temple and R. G. Williams for their invaluable generosity with their time and skills. Many thanks also to NERC for providing funding for the project and to the RAL MSF for the use of their spectroscopy facility.

References

- Blackford, D. B. and Simons, G. R.: Particle Size Analysis of Carbon Black, Particle Characterization, 4, 112–117, 1986. [74](#)
- Clapp, M. L., Miller, R. E., and Worsnop, D. R.: Frequency-dependent optical-constants of water ice obtained directly from aerosol extinction spectra, J. Phys. Chem., 99, 6317–6326, 1995. [74](#)
- Culkin, F.: The major constituents of sea water, in: Chemical Oceanography, edited by: Riley, J. P. and Skirrow, G., 1, 121–161, Academic Press, first edn., 1965. [74](#)
- Dobbie, J. S., Li, J., Harvey, R., and Chylek, P.: Sea-salt optical properties and GCM forcing at solar wavelengths, Atmos. Res., 65, 211–233, 2003. [72](#)
- DOE: Handbook of methods for the analysis of the various parameters of the carbon dioxide system in sea water, version 2, oRNL/CDIAC-74, 1994. [74](#)
- Dubovik, O., Holben, B., Eck, T. F., Smirnov, A., Kaufman, Y. J., King, M. D., Tanre, D., and

Sea salt aerosol refractive indices

R. Irshad et al.

Title Page

Abstract

Introduction

Conclusions

References

Tables

Figures

◀

▶

◀

▶

Back

Close

Full Screen / Esc

Printer-friendly Version

Interactive Discussion

**Sea salt aerosol
refractive indices**

R. Irshad et al.

Title Page

Abstract

Introduction

Conclusions

References

Tables

Figures

◀

▶

◀

▶

Back

Close

Full Screen / Esc

Printer-friendly Version

Interactive Discussion

- Slutsker, I.: Variability of absorption and optical properties of key aerosol types observed in worldwide locations, *J. Atmos. Sci.*, 59, 590–608, 2002. [72](#)
- Finlayson-Pitts, B. J. and Hemminger, J. C.: Physical chemistry of airborne sea salt particles and their components, *J. Phys. Chem. A*, 104, 11 463–11 477, 2000. [73](#)
- 5 Grainger, R. G., Lucas, J., Thomas, G. E., and Ewen, G. B. L.: Calculation of Mie derivatives, *Appl. Optics*, 43, 5386–5393, 2004. [76](#)
- Hale, G. M. and Querry, M. R.: Optical properties of water in the near infrared, *Appl. Optics*, 12, 564–568, 1973. [80](#)
- Hess, M., Koepke, P., and Schult, I.: Optical Properties of Aerosols and Clouds: The software package OPAC, *Bull. Am. Meteorol. Soc.*, 79, 831–844, 1998. [72](#)
- 10 IPCC: The Physical Basis of Climate Change, <http://ipcc-wg1.ucar.edu/wg1/wg1-report.html>, 2007. [72](#)
- Kalman, R. E.: A New Approach to Linear Filtering and Prediction Problems, *J. Basic Eng.*, 82, 35, 1960. [75](#)
- 15 King, M. D., Kaufman, Y. J., Tanre, D., and Nakajima, T.: Remote sensing of tropospheric aerosols from space: past, present and future, *Bull. Am. Meteorol. Soc.*, 80, 2229–2259, 1999. [72](#)
- Lewis, E. R. and Schwartz, S. E.: Sea Salt Aerosol Production – Mechanisms, Methods, Measurements, and Models, American Geophysical Union, 2004. [73](#), [74](#)
- 20 Lohmann, U. and Feichter, J.: Global indirect aerosol effects: a review, *Atmos. Chem. Phys.*, 5, 715–737, 2005, <http://www.atmos-chem-phys.net/5/715/2005/>. [72](#)
- Maybeck, P. S.: Stochastic Models, Estimation and Control, vol. 1, Academic Press Inc., 1979. [75](#)
- 25 Milham, M. E., Frickel, R. H., Embury, J. F., and Anderson, D. H.: Determination of optical constants from extinction measurements, *J. Opt. Soc. Am.*, 71, 1099–1106, 1981. [74](#)
- Murphy, D. M., Anderson, J. R., Quinn, P. K., McInnes, L. M., Brechtel, F. J., Kreidenweis, S. M., Middlebrook, A. M., Posfai, M., Thomson, D. S., and Buseck, P. R.: Influence of sea-salt on aerosol radiative properties in the Southern Ocean marine boundary layer, *Nature*, 392, 62–65, 1998. [73](#)
- 30 Penner, J. E., Andreae, M., Annegarn, H., Barrie, L., Feichter, J. F., Hegg, D., Jayaraman, A., Leaitch, R., Murphy, D., Nganga, J., and Pitari, G.: Aerosols, their direct and indirect effects, in: *Climate Change 2001: The Scientific Basis. Contribution of Working Group I to*

**Sea salt aerosol
refractive indices**

R. Irshad et al.

[Title Page](#)[Abstract](#)[Introduction](#)[Conclusions](#)[References](#)[Tables](#)[Figures](#)[◀](#)[▶](#)[◀](#)[▶](#)[Back](#)[Close](#)[Full Screen / Esc](#)[Printer-friendly Version](#)[Interactive Discussion](#)

the Third Assessment Report of the Intergovernmental Panel on Climate Change, edited by: Houghton, J. T., Ding, Y., Griggs, D. J., Noguer, M., van der Linden, P. J., Dai, X., Maskell, K., and Johnson, C. A., 1, 289–348, Cambridge University Press, first edn., 2001. [72](#)

Rodgers, C. D.: Inverse Methods for Atmospheric Sounding: Theory and Practice, vol. Series on Atmospheric, Oceanic and Planetary Physics - Vol. 2, World Scientific Publishing Co. Pte. Ltd., 2000. [75](#)

Rothman, L. S.: The HITRAN 2004 molecular spectroscopic database, Journal of Quantitative Spectroscopy and Radiative Transfer, 96, 139–204, 2005. [74](#), [76](#)

Savoie, D. L. and Prospero, J. M.: Particle size distribution of nitrate and sulfate in the marine atmosphere, Geophys. Res. Lett., 9, 1207–1210, 1982. [72](#)

Segelstein, D. J.: The complex refractive index of water, Master's thesis, University of Missouri – Kansas City, 1981. [80](#), [81](#)

Shettle, E. P. and Fenn, R. W.: Models for the Aerosols of the Lower Atmosphere and the Effects of Humidity Variations on Their Optical Properties, AFGL-TR-79-0214, 1979. [73](#), [77](#), [80](#), [81](#)

Thomas, G. E., Bass, S. F., Grainger, R. G., and Lambert, A.: Retrieval of aerosol refractive index from extinction spectra using a damped oscillator band model, Appl. Optics, 44, 1332–1341, 2004. [72](#), [74](#), [76](#), [78](#)

Torres, O., Bhartia, P. K., Herman, J. R., Ahmad, Z., and Gleason, J.: Derivation of aerosol properties from satellite measurements of backscattered ultraviolet radiation – Theoretical basis, J. Geophys. Res., 103(D14), 17 099–17 110, 1998. [72](#)

Twomey, S. and McMaster, K. N.: The production of condensation nuclei by crystallizing salt particles, Tellus, 7, 458–461, 1955. [72](#)

Volz, F. E.: Infrared refractive index of atmospheric aerosol substances, Appl. Optics, 11, 755–759, 1972. [73](#), [77](#), [79](#), [80](#), [81](#)

Wilson, T. R. S.: Salinity and the major elements of sea water, in: Chemical Oceanography, edited by: Riley, J. P. and Skirrow, G., 1, 365–413, Academic Press, second edn., 1975. [74](#)

Sea salt aerosol refractive indices

R. Irshad et al.

Table 1. The RH, M_{inf} , number density, particle size and spread values for the sea salt aerosols produced and measured.

RH (%)	M_{inf}	N_0 ($\times 10^6$ per cm^3)	R_m (μm)	S
0.4	2.189	9.058	0.182	1.521
22.9	1.948	6.170	0.139	1.690
29.5	1.706	0.851	0.417	1.245
38.5	1.678	0.954	0.451	1.202
48.8	1.656	0.889	0.466	1.205
68.6	1.592	0.344	0.588	1.100
74.2	1.544	0.418	0.696	1.100
76.7	1.540	0.483	0.751	1.100
86.4	1.490	0.771	0.715	1.100

Title Page

Abstract

Introduction

Conclusions

References

Tables

Figures

◀

▶

◀

▶

Back

Close

Full Screen / Esc

Printer-friendly Version

Interactive Discussion

Sea salt aerosol refractive indices

R. Irshad et al.

Table 2. Band parameters for 70% RH sea salt aerosol. The position refers to the wavenumber position of the oscillator centre, the width is the damping constant and the strength gives the maximum intensity of each band described by the CDHO model. Bands due to water are present at $\sim 1650\text{ cm}^{-1}$ and $\sim 3430\text{ cm}^{-1}$.

Position (cm^{-1})	Width (cm^{-1})	Strength (cm^{-2})
64.4	121.5	16328
483.1	222.6	234671
607.4	173.1	60835
730.6	227.2	99506
1167.6	368.1	102725
1399.8	153.3	45139
1468.8	25.1	10683
1530.3	58.5	56452
1637.5	70.9	161602
1754.5	80.5	10272
2135.0	683.5	251862
3275.8	129.7	213404
3436.6	104.7	913822
3540.6	117.2	415340
3849.4	61.8	22485
4092.2	912.8	490112
4861.0	732.2	207949

Title Page

Abstract

Introduction

Conclusions

References

Tables

Figures

◀

▶

◀

▶

Back

Close

Full Screen / Esc

Printer-friendly Version

Interactive Discussion

**Sea salt aerosol
refractive indices**

R. Irshad et al.

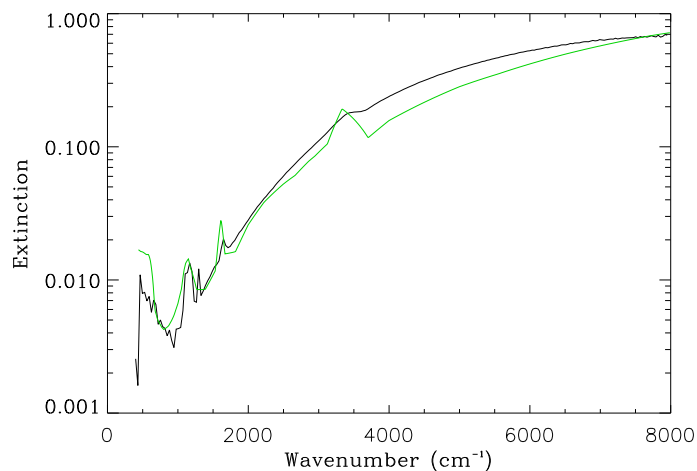


Fig. 1. Sea salt aerosol extinction from current HITRAN data (green) and from new measurements (black). Calculated assuming a particle size of $0.199\ \mu\text{m}$ and a particle number density of $9.05 \times 10^6\ \text{cm}^{-3}$.

[Title Page](#)[Abstract](#)[Introduction](#)[Conclusions](#)[References](#)[Tables](#)[Figures](#)[◀](#)[▶](#)[◀](#)[▶](#)[Back](#)[Close](#)[Full Screen / Esc](#)[Printer-friendly Version](#)[Interactive Discussion](#)

EGU

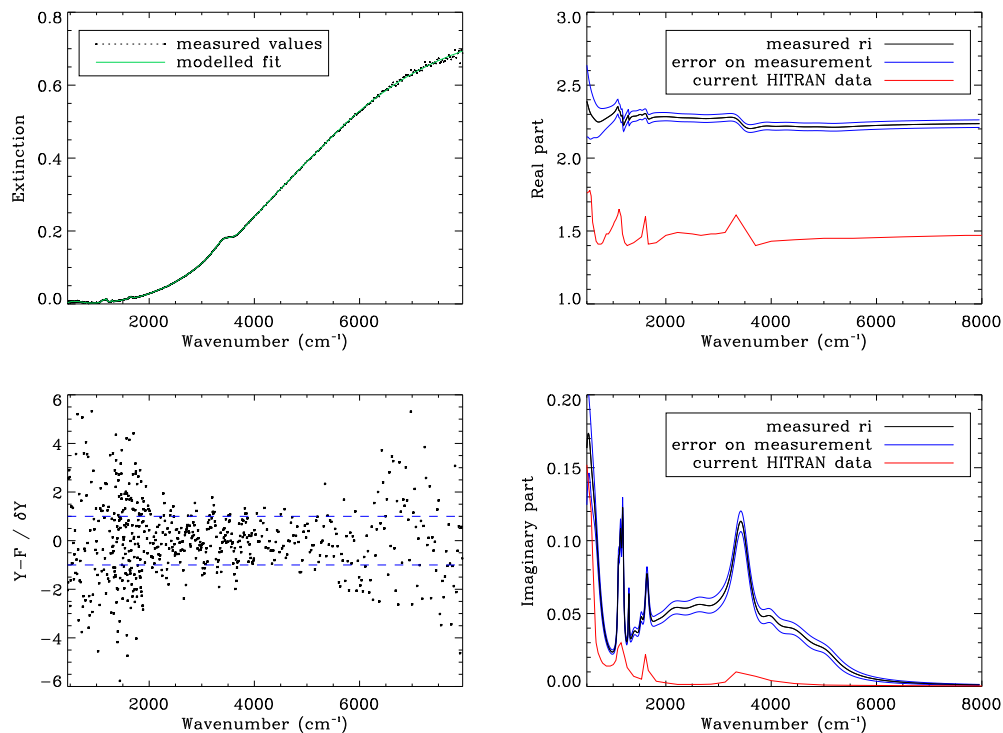


Fig. 2. Refractive index retrieval for dry sea salt aerosol. Variation of extinction with wavenumber is shown in the top left with measured values shown as black points and the modelled fit shown in green. The residual is shown in the plot to the bottom left. The right hand graphs give refractive index data retrieved from measurements in black with the error bounds in blue. Current data from HITRAN are shown in red for comparison.

Title Page

Abstract

Introduction

Conclusions

References

Tables

Figures

◀

▶

◀

▶

Back

Close

Full Screen / Esc

Printer-friendly Version

Interactive Discussion

Sea salt aerosol
refractive indices

R. Irshad et al.

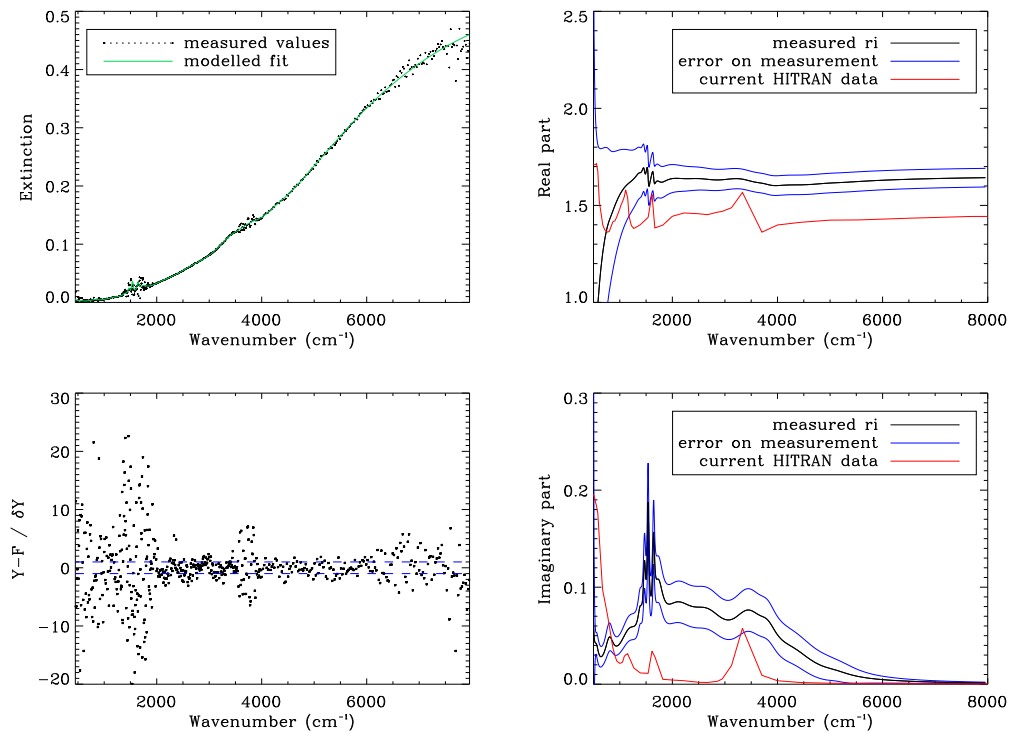


Fig. 3. Refractive index retrieval for 50% RH sea salt aerosol.

[Title Page](#)[Abstract](#)[Introduction](#)[Conclusions](#)[References](#)[Tables](#)[Figures](#)[◀](#)[▶](#)[◀](#)[▶](#)[Back](#)[Close](#)[Full Screen / Esc](#)[Printer-friendly Version](#)[Interactive Discussion](#)

Sea salt aerosol
refractive indices

R. Irshad et al.

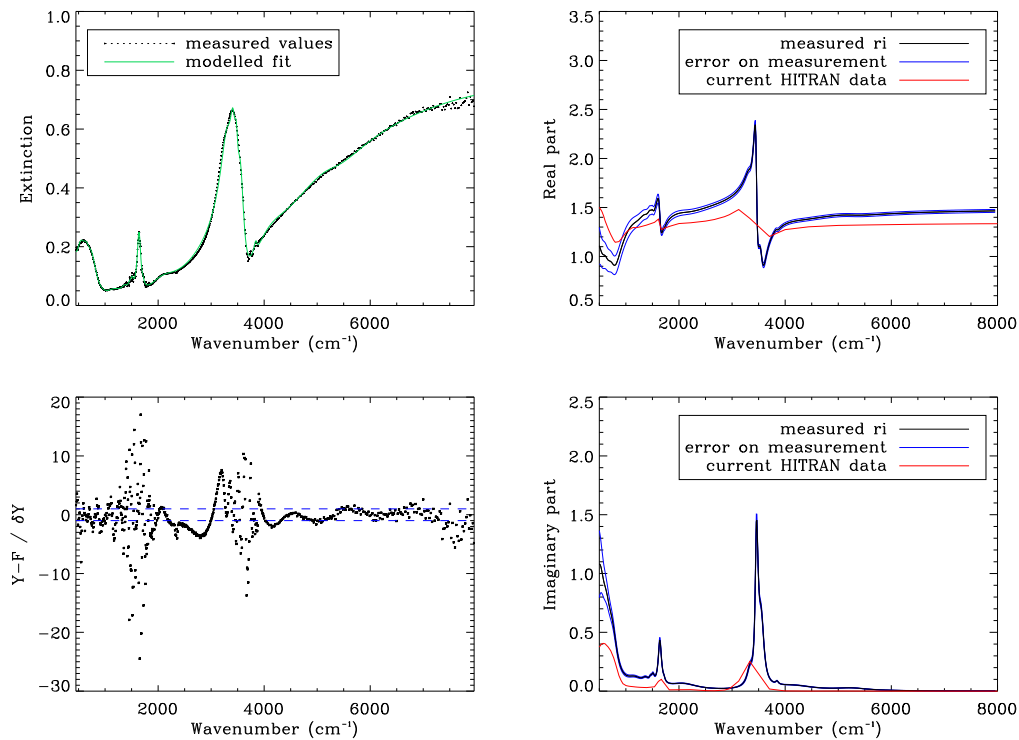


Fig. 4. Refractive index retrieval for 90% RH sea salt aerosol.

[Title Page](#)[Abstract](#)[Introduction](#)[Conclusions](#)[References](#)[Tables](#)[Figures](#)[◀](#)[▶](#)[◀](#)[▶](#)[Back](#)[Close](#)[Full Screen / Esc](#)[Printer-friendly Version](#)[Interactive Discussion](#)

EGU

**Sea salt aerosol
refractive indices**

R. Irshad et al.

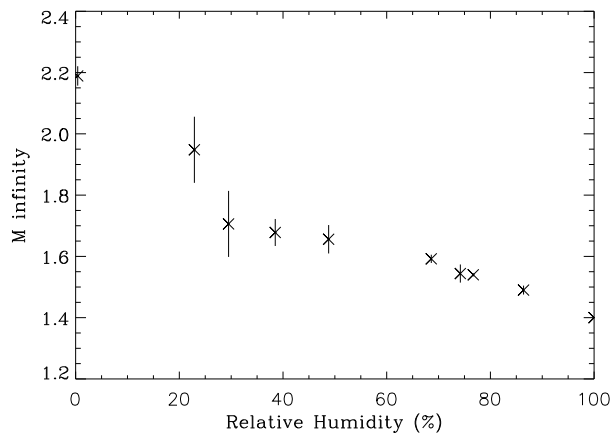


Fig. 5. Variation of refractive index at infinite wavenumber with relative humidity for sea salt aerosol. The final point at 100% RH is that of pure water and is included for comparison.

[Title Page](#)[Abstract](#)[Introduction](#)[Conclusions](#)[References](#)[Tables](#)[Figures](#)[◀](#)[▶](#)[◀](#)[▶](#)[Back](#)[Close](#)[Full Screen / Esc](#)[Printer-friendly Version](#)[Interactive Discussion](#)

EGU

Sea salt aerosol
refractive indices

R. Irshad et al.

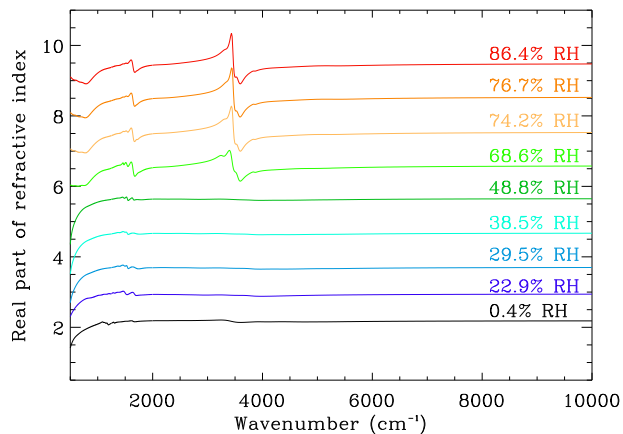


Fig. 6a. Variation of the real part of the measured refractive index, m with relative humidity. The 0.4% RH data are shown at the correct scale. Successive plots are displaced vertically by +1 unit each time.

[Title Page](#)[Abstract](#)[Introduction](#)[Conclusions](#)[References](#)[Tables](#)[Figures](#)[◀](#)[▶](#)[◀](#)[▶](#)[Back](#)[Close](#)[Full Screen / Esc](#)[Printer-friendly Version](#)[Interactive Discussion](#)

EGU

Sea salt aerosol
refractive indices

R. Irshad et al.

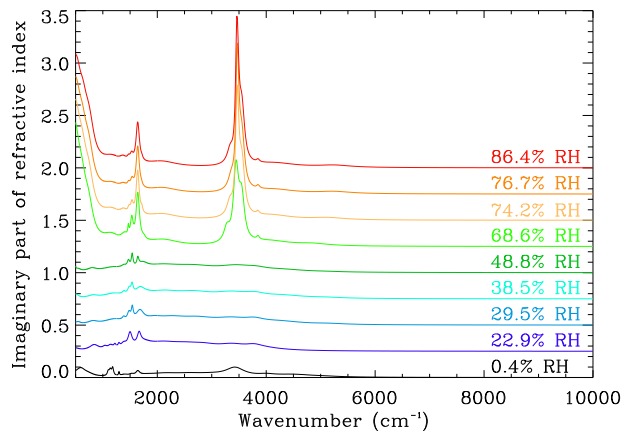


Fig. 6b. Variation of the imaginary part of the measured refractive index, k with relative humidity. The 0.4% RH data are shown at the correct scale. Successive plots are vertically displaced by +0.25 units each time.

[Title Page](#)[Abstract](#)[Introduction](#)[Conclusions](#)[References](#)[Tables](#)[Figures](#)[◀](#)[▶](#)[◀](#)[▶](#)[Back](#)[Close](#)[Full Screen / Esc](#)[Printer-friendly Version](#)[Interactive Discussion](#)

EGU

**Sea salt aerosol
refractive indices**

R. Irshad et al.

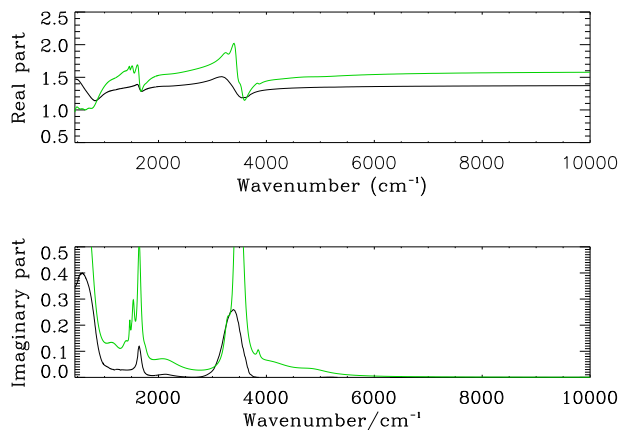


Fig. 7. Refractive index spectra of 70% RH SSA from new, direct measurements (green), and calculated from the volume mixing rules using the newly measured dry SSA refractive index (black). The real part of the refractive index is shown in the top plot, and the imaginary part in the bottom plot.

[Title Page](#)[Abstract](#)[Introduction](#)[Conclusions](#)[References](#)[Tables](#)[Figures](#)[◀](#)[▶](#)[◀](#)[▶](#)[Back](#)[Close](#)[Full Screen / Esc](#)[Printer-friendly Version](#)[Interactive Discussion](#)

EGU